Aalborg Universitet

AALBORG UNIVERSITY
DENMARK

Novel Architecture for LTE World-Phones

Barrio, Samantha Caporal Del; Tatomirescu, Alexandru; Pedersen, Gert Frølund; Morris, Art

Published in:
I E E E Antennas and Wireless Propagation Letters

DOI (link to publication from Publisher):
10.1109/LAWP.2014.2301014

Publication date:
2013

Document Version
Accepted author manuscript, peer reviewed version

Link to publication from Aalborg University

Citation for published version (APA):
Barrio, S. C. D., Tatomirescu, A., Pedersen, G. F., & Morris, A. (2013). Novel Architecture for LTE World-Phones. *I E E E Antennas and Wireless Propagation Letters*, *12*(1), 1676-1679. https://doi.org/10.1109/LAWP.2014.2301014

General rights
Copyright and moral rights for the publications made accessible in the public portal are retained by the authors and/or other copyright owners and it is a condition of accessing publications that users recognise and abide by the legal requirements associated with these rights.

- Users may download and print one copy of any publication from the public portal for the purpose of private study or research.
- You may not further distribute the material or use it for any profit-making activity or commercial gain
- You may freely distribute the URL identifying the publication in the public portal -

Take down policy
If you believe that this document breaches copyright please contact us at vbn@aub.aau.dk providing details, and we will remove access to the work immediately and investigate your claim.

Downloaded from vbn.aau.dk on: May 04, 2023

This is the author's version of an article that has been published in this journal. Changes were made to this version by the publisher prior to publication.
The final version of record is available at http://dx.doi.org/10.1109/LAWP.2014.2301014

Novel Architecture for LTE Worldphones

Samantha Caporal Del Barrio, Alexandru Tatomirescu, Gert F. Pedersen, and Art Morris

***Abstract*—The 4^{th} Generation of mobile communications (4G) came with new challenges on the antenna bandwidth and on the front-end architecture of mobile phones. This letter proposes a novel architecture overcoming these challenges. It includes narrow-band tunable antennas, co-designed with a tunable Front-End (FE). Simulations and measurements demonstrate the concept for low and high bands of the LTE frequency spectrum.**

***Index Terms*—4G mobile communication; Mobile antennas; Tunable circuits and devices; Reconfigurable architectures; Loaded antennas.**

I. Introduction

With the standardization of 4G, came along a significant broadening of the Radio Frequency (RF) spectrum. Heretofore, 4G has allocated 26 bands supporting Frequency Division Duplexing (FDD) operation, ranging from 700 MHz to 2.7 GHz [1], and new bands towards 600 MHz are being discussed [2]. The number of mobile communication bands has expanded in order to provide higher data rates. However, there is a direct correlation between the number of bands to support and the number of RF components needed on the Printed Circuit Board (PCB). Simultaneously, better data rates also initiated a need for larger screens, processors and batteries, all increasing the pressure on PCB space. Therefore, nearly no room is left to include all the components needed for global LTE roaming, and a very high degree of integration is required in future mobile phones. Moreover, the ever-increasing number of RF components on the PCB deteriorates the battery life [3].

In addition to affecting the handset FE, the spectrum expansion also impacts its antennas. Their integration is limited by fundamental limitations, that relate their impedance bandwidth to their size and efficiency [4]. Antenna concepts addressing the LTE bandwidth issue are twofold: broad-band antennas and Frequency-Reconfigurable Antennas (FRA). The main difference between these two concepts lies in the antenna natural bandwidth. Broad-band antennas are used in connection with matching networks, as in [5]–[9]; whereas FRA exhibit a narrow-band resonance that is tuned to a wide range of frequencies, as in [10]–[14]. FRA have the potential to address band proliferation, while matching previous generations antennas, volume-wise and efficiency-wise. In this contribution, a novel FE architecture is co-designed with narrow-band FRA. It addresses bands from 600 MHz to 2.17 GHz. The solution is detailed in Section II. Section III presents the dual-band antenna design, Section IV presents the simulated and measured results and Section V draws the conclusions.

S. Caporal Del Barrio, A. Tatomirescu and G. F. Pedersen are with APNet, Department of Electronic Systems, Aalborg University, DK, {scdb, ata, gfp}@es.aau.dk. A. Morris is with Wispry Inc. CA, USA, art.morris@wispry.com.

Manuscript received Dec 2, 2013.

II. Front-end Architecture

A. Conventional architecture

The RF FE groups all the RF components located between the transceiver and the antenna, including the Power Amplifier (PA), the Low Noise Amplifier (LNA), the filtering (Surface-Acoustic-Wave (SAW) filters and duplex filters) and the switches. Modern 2G/3G/4G radios typically include a broadband antenna connected to a band-selecting switch, and a FE comprising one filtering chain per band. With the band proliferation, the conventional FE architecture leads to component duplication, hence a lack of board space and an ever-increasing power consumption. An example of a conventional multi-band multi-mode RF FE is shown in Fig. 1. One can see that the main component added by 3G and 4G standards is the duplex filter, as these standards rely on full-duplex communication. One duplex filter is needed per supported band, resulting in an inefficient use of the board space and of the battery life.

With the awareness of the challenges that band expansion brought into RF FE design, also emerged a number of techniques to address it, from research groups in the academia [15], [16], [17] and from industries. The major challenge of a world-wide 4G phone is to figure out a design that will support all bands, in a small enough form factor, while improving throughput, battery life and heat dissipation. Power envelope tracking techniques have been developed [18] to reduce the power consumption and extend battery life. 3D packaging [18] has emerged in order to save PCB space, by stacking up modules. Filter banks and broadband PA are also part of the new solutions [19]. However, these techniques focus on a better integration but do not reduce the component count. In order to address LTE worldwide, the authors propose a complete shift in the design of the antenna and the FE.

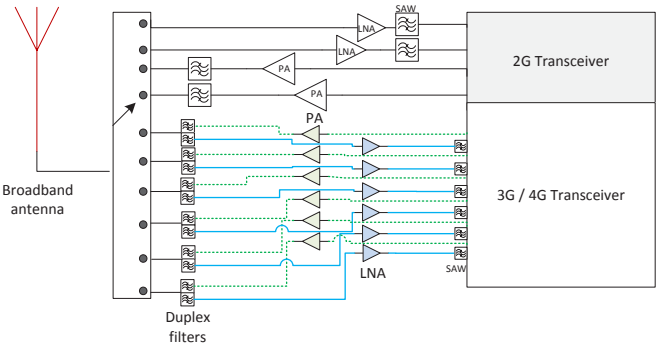

Fig. 1: Conventional 2G/3G/4G FE architecture.

B. Smart Antenna Front-End (SAFE) architecture

In this letter, the authors describe a novel FE architecture, which does not include duplex filters, main actors of the com-

Copyright (c) 2014 IEEE. Personal use is permitted. For any other purposes, permission must be obtained from the IEEE by emailing pubs-permissions@ieee.org.

This is the author's version of an article that has been published in this journal. Changes were made to this version by the publisher prior to publication.
The final version of record is available at http://dx.doi.org/10.1109/LAWP.2014.2301014

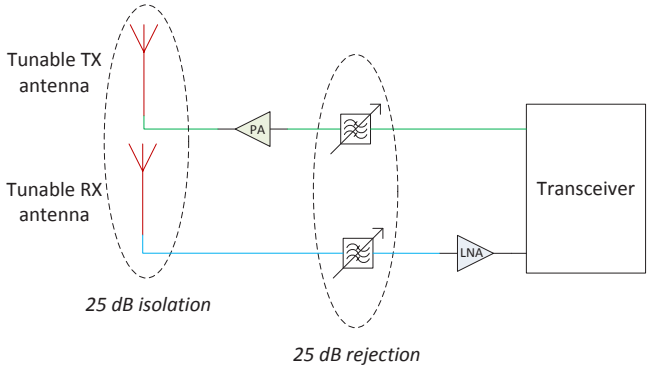

Fig. 2: Proposed SAFE architecture.

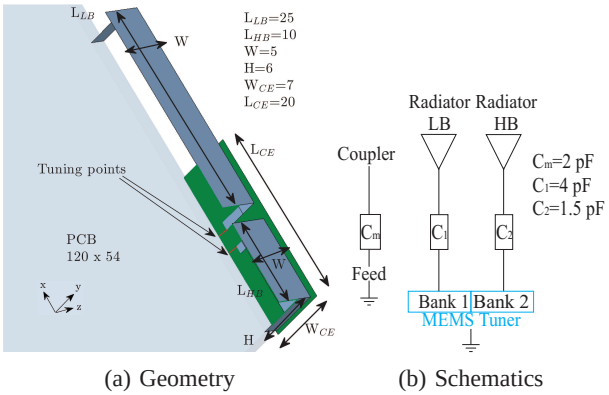

(a) Geometry (b) Schematics

Fig. 3: Antenna Design.

ponent duplication. This architecture splits the Transmitting (TX) from the Receiving (RX) paths and has been patented in [20], [21]. In order to achieve the TX/RX filtering, two distinct antennas are used in connection with two independent RF chains. The rejection typically provided by duplex filters, is provided here partly by filters in the RF chain and partly by the antennas. The key feature of this design is to separate the TX and the RX into two different antennas, each of them being narrow-band, i.e. covering only a channel instead of a full band. The authors exploit the narrow-band property of FRA for its filtering effect, in order to relax the complexity of the FE. Both the antennas and the RF filters are tunable, in order to cover the full 4G frequency spectrum. The proposed architecture is particularly advantageous in the case of bands exhibiting a very large duplex spacing, e.g. band 4 with 400 MHz. The proposed architecture is shown in Fig. 2. Eliminating the antenna switch and all the duplex filters reduces the component count by 70% compared to a conventional architecture [19], therefore reducing the complexity, the PCB area needed, the overall loss and the power consumption. Furthermore, frequency tuning ensures minimal mismatch loss, thus enhancing battery life, as the PA is not required to compensate for it anymore. The FE challenge is now shifted to the antennas and to the filters. They need to provide a duplex rejection of 25 dB in order to remove the duplex filters. This level of antenna isolation is particularly challenging at the low frequency bands (below 1 GHz), as the full board is the main radiator.

The proposed architecture was first conceptualized in 2003 [22]. Initial investigations were published in [23] and [24]. The concept was demonstrated at the high bands (1.85 GHz - 2.17 GHz) in [14]. This letter shows the performances of the duplex antenna throughout the range (600 MHz - 2.17 GHz) of the 4G spectrum, with a tunable dual-band element.

III. Antenna and Tuning Design

A. Duplex antennas

The proposed antenna design comprises a coupler connected to the feed line and two radiators, one for the high-band (HB) and one for the low-band (LB). The radiators are fed through electromagnetic coupling with the coupler. The coupler is placed 1 mm above the radiators. The radiators are connected to the tuners in order to change their electrical length, thus their resonance frequency. The antenna is a single-feed tunable dual-band antenna. The geometry of the TX antenna is depicted in Fig. 3a. The TX and RX radiators exhibit identical dimensions. The LB radiators occupy a volume of 0.75 cc each and the HB radiators occupy a volume of 0.3 cc each, leading to a total antenna volume of 2.1 cc. In order to achieve isolation of the LB radiators, the TX and RX are placed orthogonally, exciting two different modes on the ground plane. The HB radiators are isolated when placed in parallel at both ends of the ground plane, resulting from a large enough electrical distance and confined fields. High TX/RX isolation comes from having a narrow-band antenna design, i.e. an Antenna with a high Quality factor (Q_A). The Fig. 3b shows the antenna schematics and its connections to the feed and the tuner. The feed line is connected to the coupler through a matching capacitor C_m. The MEMS tunable capacitor can provide two independent banks, each exhibiting a capacitance that varies from C_{min} =1 pF to C_{max} =4.875 pF, with a resolution of 125 fF. Each of the radiators (LB and HB) is connected to one of the banks of the MEMS tunable capacitor in order to provide independent control and address all combinations of LB and HB operating frequencies. C_1 and C_2 are placed between the radiator and each bank of the MEMS tunable capacitor, in order to provide an additional degree of freedom to the voltage across the tuner, which can be critical for MEMS. However the value of C_1 and C_2 also affects the tuning range of the MEMS tunable capacitor, which also relates to the size of the antennas. Therefore a trade-off must be set between volume, acceptable voltage and tuning range, at the design stage. The proposed design is optimized for compactness.

B. MEMS Tunable capacitors

MEMS Tunable capacitors consist of a CMOS-integrated movable mechanical structures. The structure is actuated with electrostatic force to provide capacitance. Each MEMS beam is a pair of metal traces, separated by a dielectric in its on-state and by an additional air-gap in its off-state. Several beams are combined to form an array that can provide many states, i.e. a tunable capacitor. The tuner [25] used for the proposed design has two independent banks of 3.875 pF each, with tuning steps

Copyright (c) 2014 IEEE. Personal use is permitted. For any other purposes, permission must be obtained from the IEEE by emailing pubs-permissions@ieee.org.

This is the author's version of an article that has been published in this journal. Changes were made to this version by the publisher prior to publication.
The final version of record is available at http://dx.doi.org/10.1109/LAWP.2014.2301014

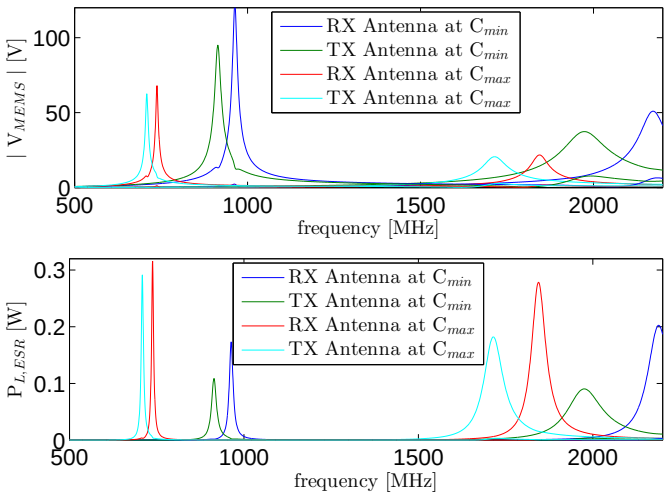

Fig. 4: Simulated voltages across the MEMS and power lost in the ESR, normalized to 1 W input power.

of 0.125 pF. The breakdown voltage is above 120 V and the Quality factor of the MEMS (Q_{MEMS}) reaches 90 at 2 GHz and 180 at 1 GHz. Each of the banks of the MEMS connect to one radiator only, in order to get full control of the operating bands.

IV. Simulated and Measured Performances

A. Voltage handling and power lost in the resistance

On the proposed design, the tuner is placed on the radiator, the furthest away from the short. This low-current location allows to best utilize the tuning range of the tuner. Nevertheless, it is also a high-voltage location, which can be an issue regarding the voltage break-down of MEMS, thus the need for C_1 and C_2. Simulations of the resulting Voltage magnitudes across the MEMS tuner ($|V_{MEMS}|$) are depicted in Fig. 4, normalized to an input power of 1 W. This figure also shows simulations of the Power lost in the Equivalent Series Resistances (ESR) of the MEMS ($P_{L,ESR}$). It is inferred that, the $P_{L,ESR}$ varies between 1.0 dB and 3.5 dB from 960 MHz to 700 MHz, depending on the operating frequency and the Q_A. Frequency dependency of the ESR loss follows the inverse relation between Q_{MEMS} and the frequency. The increasing loss, as the antenna is tuned further away from its original resonance, is due to an increasing Q_A of the element.

B. Tunability and efficiency

A printed circuit board with the two single RX and TX chains, corresponding to the schematic in Fig. 2, is built; and shown in Fig. 5. Due to manufacturing issues, the board used for this investigation can only support one bank per MEMS tunable capacitor. Therefore the antennas were measured independently in the following way: the HB radiators were shunt with a high-Q fixed capacitor during the LB measurements, and vice-versa. The following measurements reflect the tunable antenna performance alone, with direct traces to the antenna feeds omitting the RF chains, in order to assess the feasibility of the solution and provide antenna efficiency values

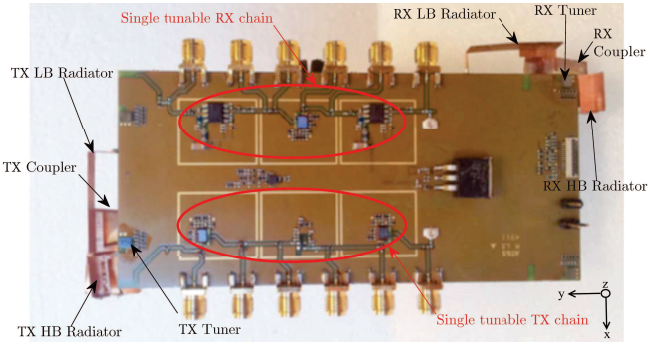

Fig. 5: Measurement board.

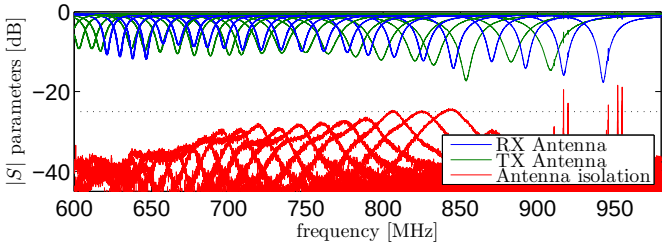

Fig. 6: Measured |S| parameters of the LB antennas.

in challenging bands. Both TX and RX antennas are swept simultaneously. The measured |S| parameters of the low-band antennas are shown in Fig. 6. The bandwidth of the TX and the RX antennas shrink from 19 MHz and 14 MHz respectively to 6 MHz, as they are tuned to the 600 MHz region. The figure shows coverage for the LTE bands 5-6, 8, 12, 17-20, 26-29. The high-band antennas are designed for band 1,2,4 and the measurement results are shown in Fig. 7. In order to efficiently cover LTE band 7, a smaller value of C_{min} is required for the tuner. In order to show the tunability of the low band until 600 MHz, C1 was omitted. The plots show impedance coverage at -6 dB of all frequencies of the targeted bands. Indeed the tuning resolution depends on the minimum step of the tuner and its placement on the antenna design. In both figures, it can also be observed that the isolation between the TX and RX antennas is above 25 dB. The loaded Q_A of the mock-up is shown for the LB antennas. The measured Q_A of the TX and the RX antennas exhibit an increase of 57% and 55% from their initial value respectively. The RX antenna exhibits higher Q_A values than the TX, resulting from its location on the board, and the mode it excites. The Q_A values at the HB show a similar trend, with peak values at 70 for the RX and 50 for the TX. For the sake of concision, the Q_A is only shown for LB, being the most challenging frequencies to address on a small terminal.

The mock-up was measured in Satimo Star-Lab to calculate its total efficiency (η_T) with 3D pattern integration technique. TX values are summarized in Table I. The RX antenna exhibits a similar trend, worsened by 1 dB due to a higher Q_A. η_T including tuner loss are in-line with η_T of todays market antennas alone [26], [27]. Using narrow-band antennas here leads to reducing the antenna volume while keeping a high efficiency.

Copyright (c) 2014 IEEE. Personal use is permitted. For any other purposes, permission must be obtained from the IEEE by emailing pubs-permissions@ieee.org.

This is the author's version of an article that has been published in this journal. Changes were made to this version by the publisher prior to publication.
The final version of record is available at http://dx.doi.org/10.1109/LAWP.2014.2301014

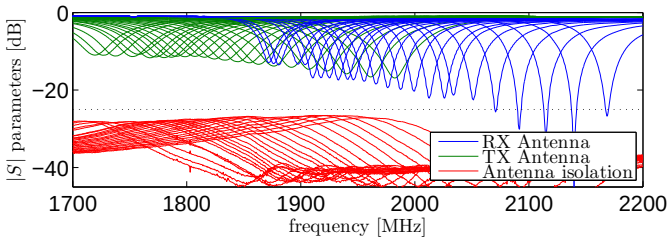

Fig. 7: Measured |S| parameters of the HB antennas.

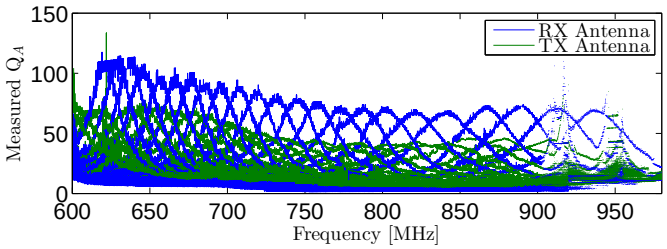

Fig. 8: Measured Q_A of the LB antennas.

TABLE I: Measured η_T of the TX antenna

f [MHz]	1980	1710	900	800	700	600
η_T [dB]	-3	-4	-3	-4	-5	-7

V. Conclusion

Radio spectrum and PCB area are the two most precious entities in the mobile phone landscape nowadays. The user's demand for mobile data drives the RF FE content. However, the number of bands required worldwide leads to high component duplication and PCB space has become an issue. Moreover, antennas covering a large bandwidth are typically large and difficult to fit into thin and modern mobile phone designs. A novel architecture is proposed in this letter, combining a new approach for the FE design and for the antenna design. The implementation of tunable, narrow-band and highly isolated antennas will save space and power consumption, leading to an efficient design. A mock-up was built, as a proof-of-concept of the proposed architecture. Antenna duplex isolation above 25 dB was achieved. The forthcoming challenges for this architecture appear when one considers Multiple-Input Multiple-Output (MIMO) and Carrier Aggregation (CA) support, required for 4G. Supporting MIMO with the proposed architecture requires to double the number of antennas on the PCB, especially adding a RX RF chain and a RX antenna for today's market requirements. The main challenge is to simultaneously decouple both TX/RX links and both RX. Inter-band LB/HB CA is supported with the proposed design, with the independent tuning of each radiator. However, LB/LB and HB/HB CA require a dual-resonant design of each of the radiators. The proposed mock-up exhibits a nominal total efficiency, resulting from the conductive loss of the antenna and the Q_{MEMS}.

Acknowledgment

The work is supported by the Smart Antenna Front End (SAFE) Project within the Danish National Advanced Technology Foundation, High Technology Platform.

References

[1] 3GPP TS 36.101, "LTE; Evolved Universal Terrestrial Radio Access (E-UTRA); User Equipment (UE) radio transmission and reception," 2013.
[2] Www.dailywireless.org, "600 MHz Auction Speculation," 2013.
[3] D. Vye, "The Economics of Handset RF Front-end Integration," 2010.
[4] R. F. Harrington, "Effect of Antenna Size on Gain, Bandwidth, and Efficiency," *Journal of Research of the National Bureau of Standards-D. Radio Propagation*, vol. 64D, no. 1, pp. 1–12, 1960.
[5] D. Manteuffel and M. Arnold, "Considerations for Reconfigurable Multi-Standard Antennas for Mobile Terminals total efficiency :," in *Antenna Technology: Small Antennas and Novel Metamaterials, 2008. iWAT 2008. International Workshop on*, pp. 231–234, 2008.
[6] L. Huang and P. Russer, "Electrically Tunable Antenna Design Procedure for Mobile Applications," *IEEE Transactions on Microwave Theory and Techniques*, vol. 56, pp. 2789–2797, Dec. 2008.
[7] R. Valkonen, J. Ilvonen, and P. Vainikainen, "Naturally Non-Selective Handset Antennas with Good Robustness Against Impedance Mistuning," in *European Conference on Antennas and Propagation (EuCAP)*, pp. 796–800, 2011.
[8] R. Valkonen, M. Kaltiokallio, and C. Icheln, "Capacitive Coupling Element Antennas for Multi-Standard Mobile Handsets," *IEEE Transactions on Antennas and Propagation*, vol. 61, no. 5, pp. 2783–2791, 2013.
[9] R. Valkonen, C. Luxey, J. Holopainen, C. Icheln, and P. Vainikainen, "Frequency-reconfigurable mobile terminal antenna with MEMS switches," in *Antennas and Propagation (EuCAP), 2010 Proceedings of the Fourth European Conference on*, pp. 1–5, 2010.
[10] M. G. S. Hossain and T. Yamagajo, "Reconfigurable Printed Antenna for a Wideband Tuning," in *European Conference on Antennas and Propagation (EuCAP)*, vol. 1, pp. 1– 4, 2010.
[11] H. Li, J. Xiong, Y. Yu, and S. He, "A Simple Compact Reconfigurable Slot Antenna With a Very Wide Tuning Range," *IEEE Transactions on Antennas and Propagation*, vol. 58, no. 11, pp. 3725–3728, 2010.
[12] Y. Tsutsumi, M. Nishio, S. Obayashi, H. Shoki, T. Ikehashi, H. Yamazaki, E. Ogawa, T. Saito, T. Ohguro, and T. Morooka, "Low Profile Double Resonance Frequency Tunable Antenna Using RF MEMS Variable Capacitor for Digital Terrestrial Broadcasting Reception," in *IEEE Asian Solid-State Circuits Conference*, pp. 125–128, 2009.
[13] S. K. Oh, H. S. Yoon, and S. O. Park, "A PIFA-Type Varactor-Tunable Slim Antenna With a PIL Patch Feed for Multiband Applications," *Antennas and Wireless Propagation Letters*, vol. 6, no. 11, pp. 103–105, 2007.
[14] J. R. De Luis, A. Morris, Q. Gu, and F. de Flaviis, "Tunable Duplexing Antenna System for Wireless Transceivers," *IEEE Transactions on Antennas and Propagation*, vol. 60, pp. 5484–5487, Nov. 2012.
[15] T. Nesimoglu, "A Review of Software Defined Radio Enabling Technologies," in *Microwave Symposium (MMS), 2010 Mediterranean*, pp. 87–90, 2010.
[16] I. Dufek, "Concept of the Tunable Filter Unit for Agile Mobile Handsets," in *Loughborough Antennas and Propagation Conference (LAPC)*, no. November, pp. 5–8, 2012.
[17] H. Okazaki, T. Furuta, K. Kawai, Y. Takagi, A. Fukuda, and S. Narahashi, "Reconfigurable RF Circuits for Future Multi-Mode Multi-Band Mobile Terminals," in *2013 International Symposium on Electromagnetic Theory*, pp. 432–435, 2013.
[18] P. Carson and S. Brown, "White paper: Less is More - The New Mobile RF Front-End," 2013.
[19] B. D. Pilgrim, "White paper: Simplifying RF front-end design in multiband handsets," 2008.
[20] M. B. Knudsen, et. al., "Impedance Tuning of Transmitting and Receiving Antennas ," U.S. Patent 8232925, July 31, 2012.
[21] M. B. Knudsen, et. al., "Wireless Communication Device Antenna with Tuning Elements," U.S. Patent 20100302123, Dec. 2, 2010.
[22] A. James, "Reconfigurable Antennas for Portable Wireless Devices," *IEEE Antennas and Propagation Magazine*, vol. 45, no. 6, pp. 148–154, 2003.
[23] M. Pelosi, M. B. Knudsen, and G. F. l. Pedersen, "Multiple Antenna Systems with Inherently Decoupled Radiators," *IEEE Transactions on Antennas and Propagation*, vol. 60, no. 2, pp. 503–515, 2012.
[24] O. N. Alrabadi, A. D. Tatomirescu, M. B. Knudsen, M. Pelosi, and G. F. Pedersen, "Breaking the Transmitter-Receiver Isolation Barrier in Mobile Handsets with Spatial Duplexing," *IEEE Transactions on Antennas and Propagation*, vol. 61, no. 4, pp. 2241–2251, 2013.
[25] WiSpry Tunable Digital Capacitor Arrays (TDCA), "http://www.wispry.com/products-capacitors.php."
[26] S. Caporal, D. Barrio, and G. F. Pedersen, "Correlation Evaluation on Small LTE Handsets," in *Vehicular Technology Conference (VTC Fall)*, pp. 1–4, 2012.
[27] A. Tatomirescu and G. F. Pedersen, "Body-loss for Popular Thin Smart Phones," in *European Conference on Antennas and Propagation (EUCAP)*, pp. 3754–3757, 2013.

Copyright (c) 2014 IEEE. Personal use is permitted. For any other purposes, permission must be obtained from the IEEE by emailing pubs-permissions@ieee.org.